

A Low-Cost Active Control Multi-Fan Turbulence Wind Tunnel with an Embedded System to Generate Natural Wind

Haruka Kikuchi, Hiroyuki Matsubara, Parnravee Pornthisarn, Kazuhiko Toshimitsu

Department of Information and Systems Engineering, Fukuoka Institute of Technology, Fukuoka, Japan
Email: toshimitsu@fit.ac.jp

How to cite this paper: Kikuchi, H., Matsubara, H., Pornthisarn, P. and Toshimitsu, K. (2019) A Low-Cost Active Control Multi-Fan Turbulence Wind Tunnel with an Embedded System to Generate Natural Wind. *Open Journal of Fluid Dynamics*, 9, 158-167. <https://doi.org/10.4236/ojfd.2019.92011>

Received: April 24, 2019

Accepted: June 15, 2019

Published: June 18, 2019

Copyright © 2019 by author(s) and Scientific Research Publishing Inc. This work is licensed under the Creative Commons Attribution International License (CC BY 4.0). <http://creativecommons.org/licenses/by/4.0/>



Open Access

Abstract

This paper describes a new actively controlled multi-fan wind tunnel that generates natural wind as a type of turbulence wind tunnel at a reduced cost. The driving section of the wind tunnel has 100 PC cooling fans that are controlled by an original embedded system. The fluctuating velocity wind is successfully generated with a mean velocity of 7 m/s and two turbulent intensities of 2% and 3% based on Karman's power spectrum density function. The case of 2% has the integral scales of 5 m, 10m and 20 m, and the case of 3% has the integral scales of 3 m, 6 m and 15 m with a turbulence grid. In particular, the wind with the turbulent intensity of 2% satisfies the Kolmogorov's $-5/3$ multiplication rule of inertial subrange with the frequency range from 0.01 Hz to 2.0 Hz. Consequently, the new wind tunnel can be used for studying engineering technology and research regarding conditions with natural wind.

Keywords

Wind Tunnel, Natural Wind, Flow Control, Embedded System, Turbulence, Wind Turbine

1. Introduction

Turbulent flow is a significant concern within engineering technology and fluid dynamics research. Wind turbine design and environmental assessments of natural wind and buildings in urban development are typical real-world applications of such related research. For these applications, it is important that we can produce the turbulent flow experimentally and clarify the influence of turbulence on the research objects. Therefore, various types of turbulence wind tun-

nels have been developed to generate the turbulent flow for the research purposes. Makita [1], for instance, surveyed previous research of turbulence wind tunnels. A multi-fan actively controlled turbulence wind tunnel is one type of turbulence wind tunnel which is suitable for generating natural wind. The development of the wind tunnel was started in the 1990s. For instance, Nishi, A., Kikugawa, H., Matsuda, Y. and Tashiro, D. [2] developed the wind tunnel for obtaining several turbulence parameter profiles in both longitudinal and vertical directions through controlled 99 DC servo motors. While, Nomura, T., Yamagata, T. and Kimura, K. [3] improved the same kind of the wind tunnel driven by multi AC servo motors. Recently, Ozono, S., Miyagi, H. and Wada, K. [4] proposed an efficient driving mode for generating high-Reynolds number isotropic turbulence, a new driving mode (“active grid mode”) is attempted where the active and inactive fans are grid-like arranged by 99 small fans. Furthermore, Cao, S. and Cao, J. [5] briefly introduced a newly developed multiple-fan wind tunnel which is designed to control turbulence to assist the study of turbulence effects. Wang, J.Y, Meng, Q. H., Luo, B. and Zeng, M. [6] presented a new type of active controlled multiple-fan wind tunnel. The wind tunnel consists of swivel plates and arrays of direct current fans, and the rotation speed of each fan and the shaft angle of each swivel plate can be controlled independently for simulating different kinds of outdoor wind fields. According to these references, the multi-fan wind tunnels have been developed for generating desired natural wind. However, the system becomes more complex at high cost.

This paper shows that the possibility of the low-cost multi-fan actively controlled turbulence wind tunnel which consists of driving PC cooling fans and an original embedded system. One purpose of using the low-cost wind tunnel is to easily clarify the influence of natural wind on the performance of a wind turbine through a laboratory-based experiment. Therefore, we used the multi-fan type wind tunnel as the generator of natural wind to investigate the effect of turbulent flow on the wind turbine performance. Specifically, this paper shows the composition of the new wind tunnel and the characteristics of the generated natural wind. Furthermore, we clarify the generating conditions and reproducibility of the real natural wind with our original procedure method.

2. Wind Tunnel

Figure 1 shows the schematics of the new wind tunnel. Location A and B are the velocity measurement points of steady wind. The cross section is 61 cm squared. The driving section consists of 100 PC cooling fans. Usually, servo-motors are suitable for driving the fans to control the wind tunnel. However, the multi-fan wind tunnel requires as many servo-motors as driving fans, and the cost of a servomotor per driving fan is over 10 times as expensive as a PC fan. The driving section of this wind tunnel needs 50 driving motors. Therefore, this wind tunnel can be made at about one-tenth of the expense of the servomotor driving method. However, controlling the rotation of the PC fans is more difficult than the servomotor driving. Hence, we have to devise a way to produce natural wind on the control system.

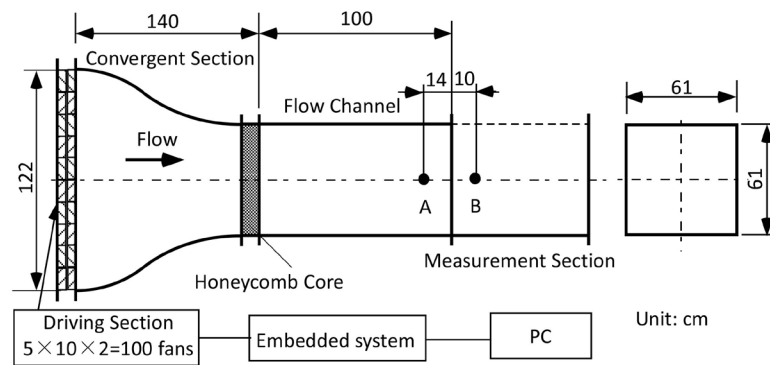


Figure 1. Schematics of multi-fan type wind tunnel.

The horizontal and vertical contraction ratios in the convergent section are 1 and 2 respectively. **Figure 2** and **Figure 3** show the configuration and control flow chart of the controlling fan system. To control the wind, we use ARM embedded system (STMicroelectronics NUCLEO-F446RE and STM32F446RE) for minimizing delay time and real-time controlling capability. The control program can be compiled by the open source Mbed compiler on web. The Pulse Width Modulation (PWM) with 12 VDC controls the PC fans electrically. The PWM controller consists of four NXP PCA 9685s with 16 channels, which can generate PWM waveforms. The power amplifiers are designed originally and amplify the PWM waveform to 12 VDC and 1.3 A for each channel. When the 100 PC fans start instantaneously, a large current of 130 A is required. Furthermore, the controlling voltage drops due to the electric wiring path and wiring length from the power amplifier to the PC fan. Therefore, we divide the electric load of power consumption into six 500 W class ATX power supplies with 12 V lanes (up to 38 A/unit). As a result, this wind tunnel can be used with an ordinary power supply of about 100 V and 20 A.

3. Characters of the Wind Tunnel

3.1. Steady Wind

Firstly, we clarify the steady wind velocity distribution as the basic characteristic of the wind tunnel. The velocity distribution on the cross-section is measured as shown points along x , y , $xy+$ and $xy-$ directions in **Figure 4**. The measurement positions of the wind tunnel are shown as A (14cm upstream from the wind tunnel ended with a wind tunnel wall) and B (10cm downstream without upper, left and right wind tunnel walls) in **Figure 1**. Here, in order to change the turbulent intensity of the generated natural wind, we use the removable wooden turbulence grid as shown in **Figure 5**. It is set at the next downstream side of the honeycomb rectifier. This turbulence grid is made of a wooden 9 mm squared pillar with an 83% open area ratio. In consideration of the influence of this grid on steady flow, the wind velocity distribution of steady wind is measured with and without the turbulence grid. We confirm that the average wind speed distribution hardly changed with or without the turbulence grid, and the uniformity

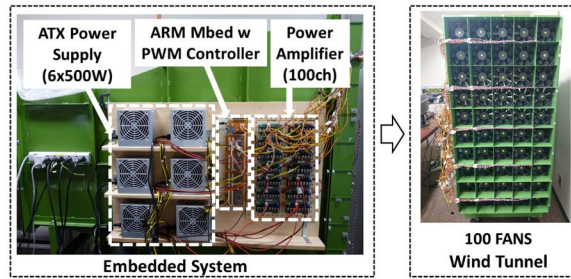


Figure 2. Photographs of the embedded system and 100 fans.

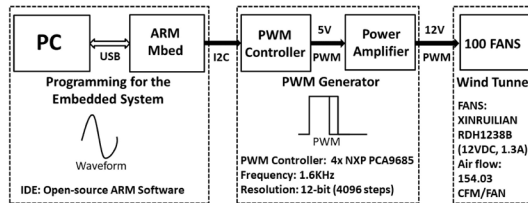


Figure 3. The embedded system to control 100 fans.

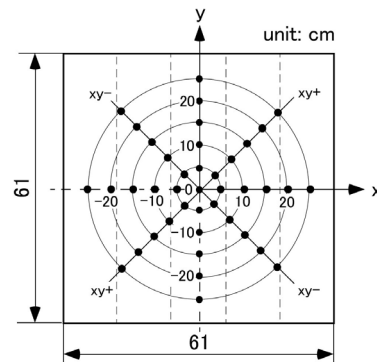


Figure 4. Measurement point on cross section A and B for steady wind.

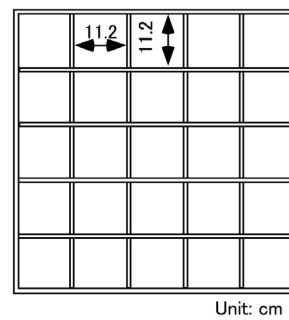


Figure 5. Turbulence grid.

of the velocity distribution is the same or more uniform than one with the turbulence grid. Figure 6 and Figure 7 show the steady velocity distribution with the turbulence grid. The effect of the measurement positions A and B is very small. The wind velocities near the wall of the wind tunnel drop from the wall effect. However, the deviation from the average wind velocity is small. For example, there are up to 1.2% and 0.9% with the average wind velocity of 7.3 m/s

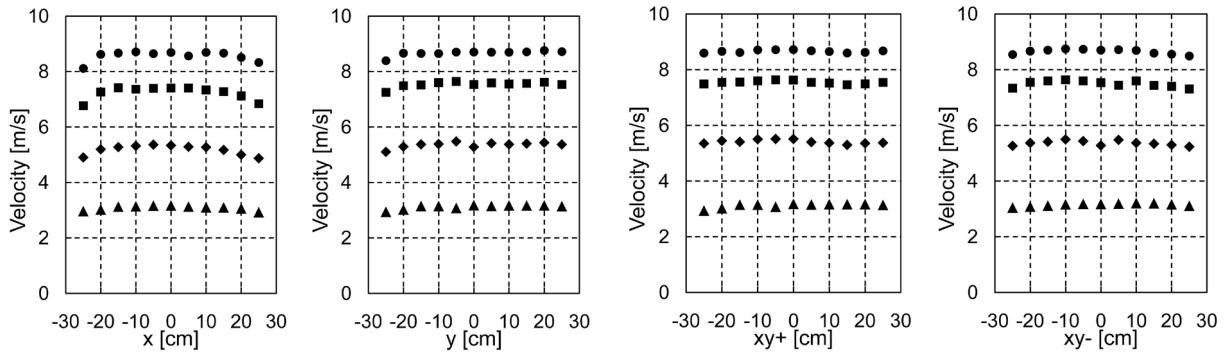


Figure 6. The velocity distributions of steady wind on the cross section A with turbulence grid.

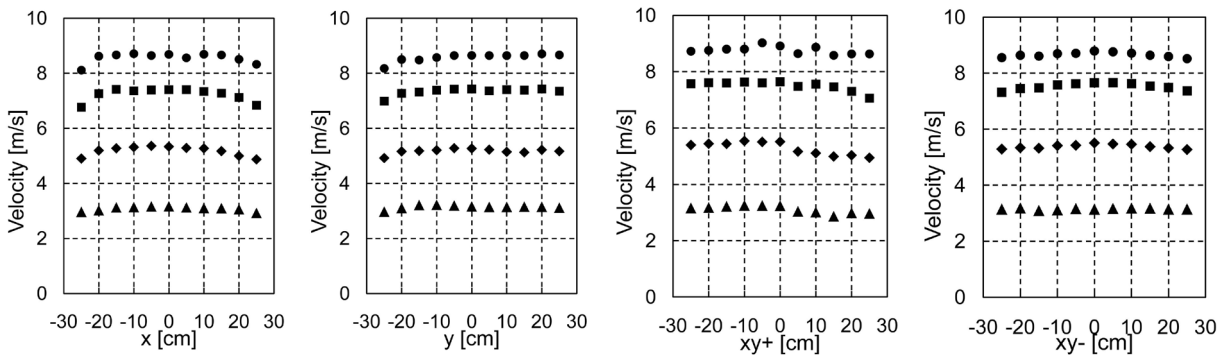


Figure 7. The velocity distributions of steady wind on the cross section B with turbulence grid.

in the range of -15 cm to 15 cm on the x and y axes at B, respectively. Since we plan the research using a wind turbine with a rotor of 20 cm diameter (-10 cm to 10 cm), the uniformity is sufficient enough to study. In addition, the wind tunnel can generate the mean steady wind velocity from 3 m/s to 8.6 m/s.

3.2. Natural Wind

We verified that the steady wind can be generated as almost uniform velocity distribution on the cross section A and B in Section 3.1. This is required as the fundamental character of the wind tunnel for testing wind turbine performance. Next, we will discuss about generating natural wind with fluctuating velocity.

The prescribed wind tunnel generates arbitrary artificial natural wind that is based on Kármán’s power spectral density function (PSD) [7] [8] [9] as Equations (1) and (2).

$$S_u(f) = 4I^2LU \frac{1}{\left[1 + 70.8 \left(\frac{fL}{U}\right)^2\right]^{\frac{5}{6}}} \tag{1}$$

$$I = \frac{\sigma}{U} \tag{2}$$

Here, S_u , f , U , I and L denote the power spectral density function [m^2/s], frequency [Hz], mean wind velocity [m/s], turbulent intensity and integral scale, respectively. The turbulent intensity I is defined by Equation (2) with standard

deviation σ of fluctuating wind velocity. Here, we use the integral scale means as a statistical parameter representing the mean turbulent scale under Taylor's hypothesis of "frozen turbulence". Hence, L cannot be directly connected to the wind turbine size.

Figure 8 shows the procedure for generating artificial natural wind by wind tunnel. Firstly, we apply inverse FFT to modified Kármán's PSD under the assumption of a random phase. Then the time series velocity for ten minutes to control the PC fans is generated as shown in the upper right graph of **Figure 8**. Next, we operate the wind tunnel using the control velocity data. Lastly, the artificial natural wind, which is measured by the hot wire anemometer, can be generated as seen in the lower left graph of **Figure 8**.

Figure 9 illustrates the procedure of determining the turbulent intensity I and integral scale L of the generated natural wind. The generated wind PSD is made

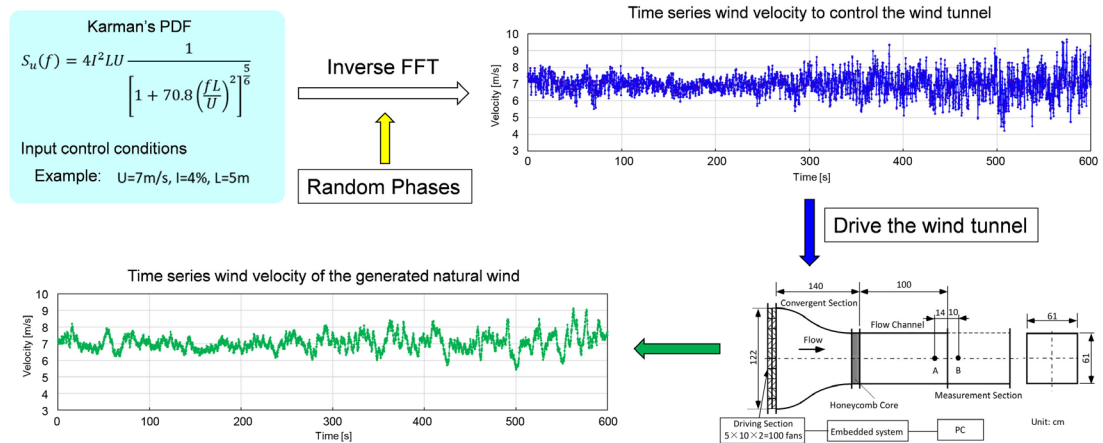


Figure 8. Procedure to generate natural wind by wind tunnel.

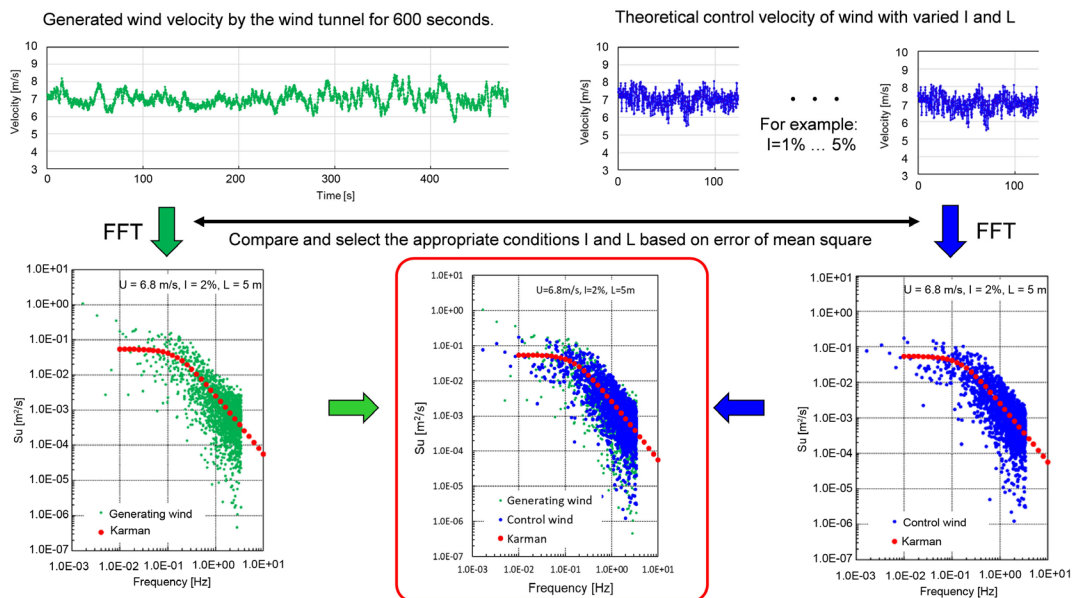


Figure 9. Procedure to determine turbulent intensity and integral scale of generated natural wind.

through FFT analysis of the time series velocity as shown in the two left green graphs. On the other hand, the theoretical control PSDs are made from the time series velocity data with changing I and L to control the wind tunnel, which are shown in the right blue symbol graphs in **Figure 9**. We can estimate the I and L of the generated wind through the minimum difference of the two PSDs based on mean square, like as seen in the lower middle graph with a red frame. **Table 1** summarizes these conditions of control and generated natural winds.

Figures 10-15 show PSDs of the generated natural wind with mean velocity of about 7 m/s as No.1 to 6 in **Table 1**, respectively. The left and middle figures show the PSDs of theoretical and experimental generated natural wind. The right figures show the composite PSDs to compare them. In addition, the red circle symbol shows Kármán's PSD.

In the cases without the turbulence grid (**Figures 10-12**), the theoretical and experimental wind PSDs are in good agreement at the turbulent intensity, $I = 2\%$. In particular, the PSDs satisfy the Kolmogorov's $-5/3$ multiplication rule of inertial subrange with frequency from 0.01 Hz to 2.0 Hz.

While the turbulence grid increases turbulent intensity by about 1% (*i.e.* $I = 3\%$) as shown in **Figures 13-15**. The theoretical and experimental wind PSDs are in good agreement in the range of the frequency from 0.01 Hz to 1.0 Hz with $I = 3\%$. The turbulence grid raises PSD in the range of over frequency of 1.0 Hz, and experimental PSD is larger than theoretical PSD. This result is commonly known as the turbulence grid effect. The actual natural wind of the offshore wind at Fukushima, Japan has this character [10]. Hence, it is implied that these winds with turbulence grid can simulate the same kind of the offshore natural wind. In addition, if the mean wind velocity is reduced, the natural winds with larger turbulent intensity can be generated. This is because the turbulent intensity is defined by Equation (2).

Consequently, the natural winds can be generated as the conditions of **Table 1** by the low-cost wind tunnel, which almost meet the theoretical conditions based

Table 1. Conditions of control and generated natural winds.

No.	Control conditions			Generated wind conditions		
	U [m/s]	I [%]	L [m]	U [m/s]	I [%]	L [m]
Without the turbulence grid						
1	7.0	4	5	6.8	2	5
2	7.0	4	10	6.7	2	10
3	7.0	4	20	7.0	2	20
With the turbulence grid						
4	6.9	4	5	7.0	3	3
5	6.9	4	10	7.0	3	6
6	7.0	4	20	7.0	3	15

on Karman's PSD. Hence, these natural winds are useful to investigate the influence of natural wind on the performance of the wind turbines through a laboratory-based experiment.

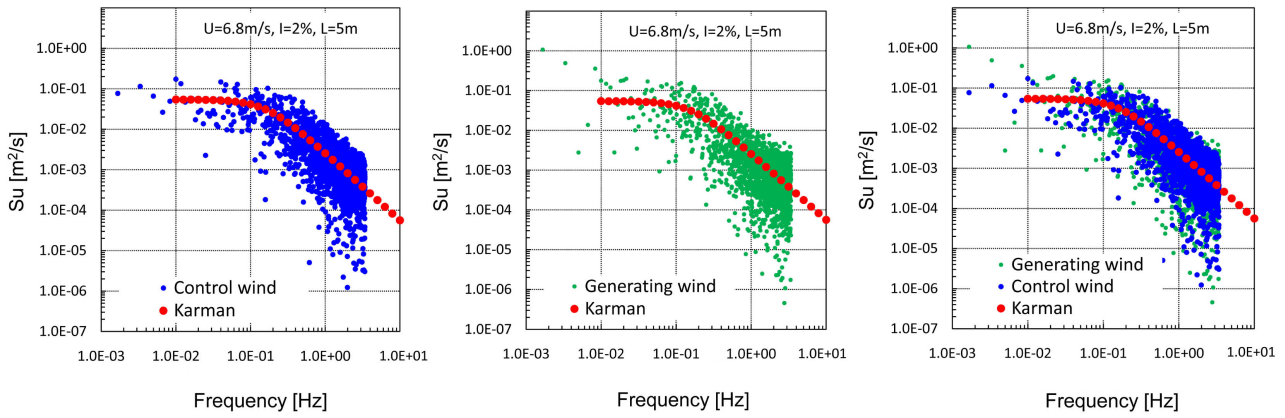


Figure 10. Comparison of PSD of control and generated wind without the turbulence grid at $U = 6.8$ m/s, $I = 2\%$ and $L = 5$ m (Left: control, middle: generated, right: composite).

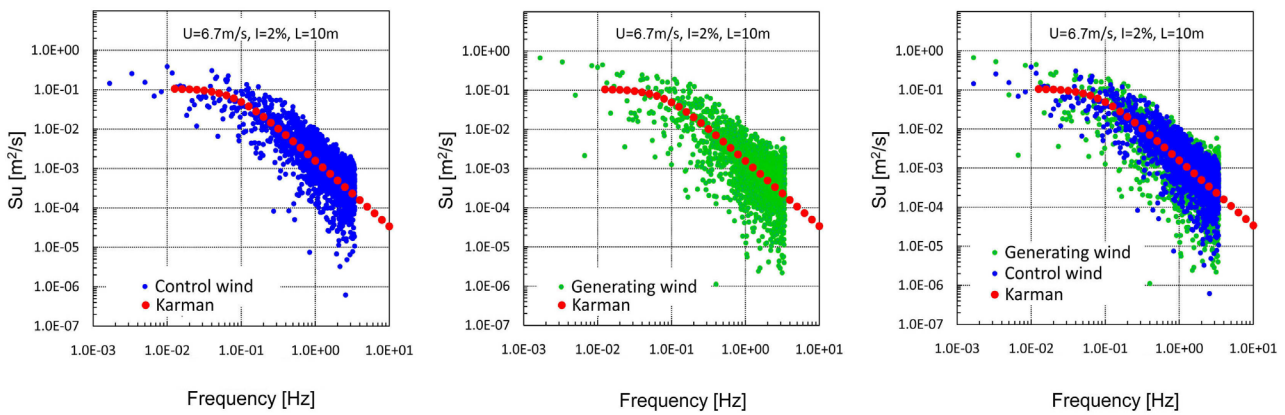


Figure 11. Comparison of PSD of control and generated wind without the turbulence grid at $U = 6.7$ m/s, $I = 2\%$ and $L = 10$ m (Left: control, middle: generated, right: composite).

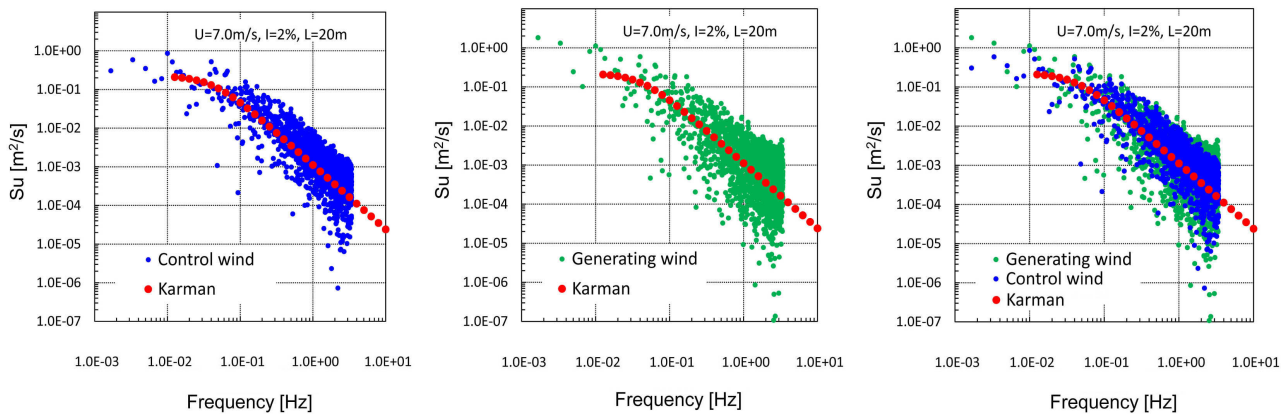


Figure 12. Comparison of PSD of control and generated wind without the turbulence grid at $U = 7.0$ m/s, $I = 2\%$ and $L = 5$ m (Left: control, middle: generated, right: composite).

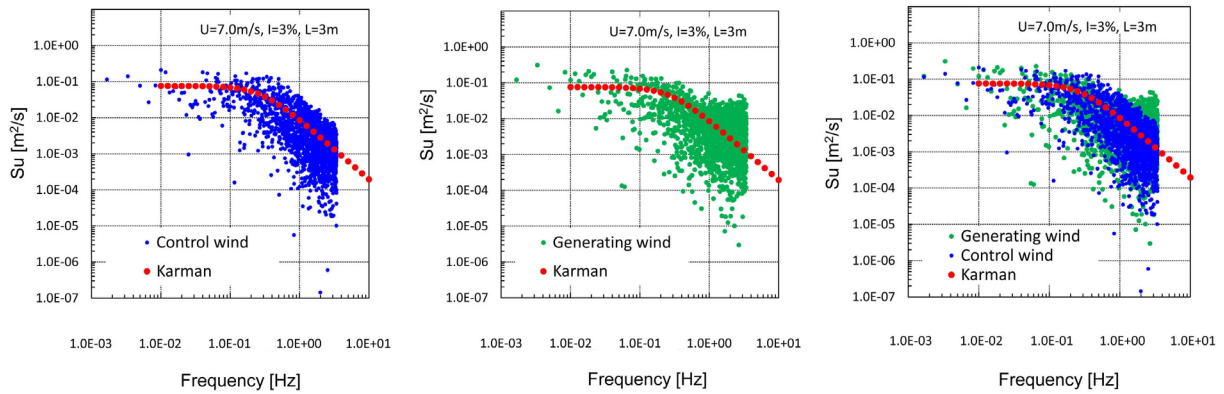


Figure 13. Comparison of PSD of control and generated wind with the turbulence grid at $U = 7.0$ m/s, $I = 3\%$ and $L = 3$ m (Left: control, middle: generated, right: composite).

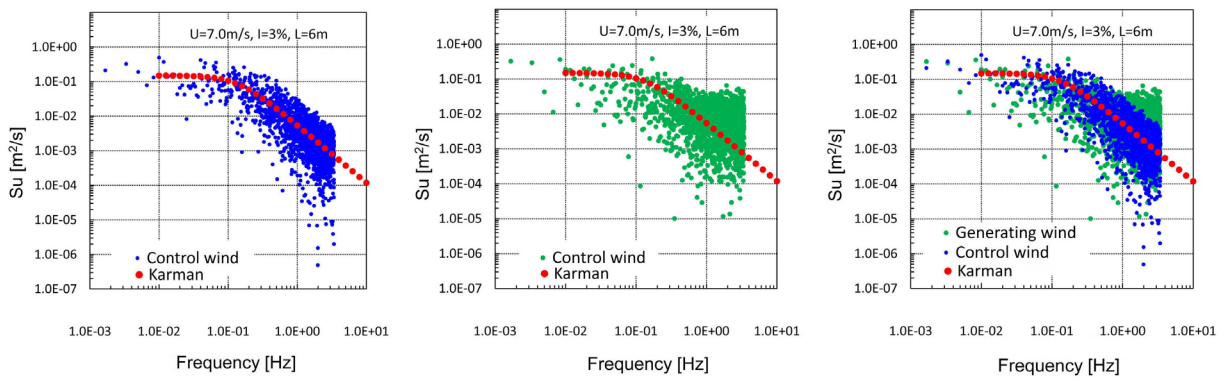


Figure 14. Comparison of PSD of control and generated wind with the turbulence grid at $U = 7.0$ m/s, $I = 3\%$ and $L = 6$ m (Left: control, middle: generated, right: composite).

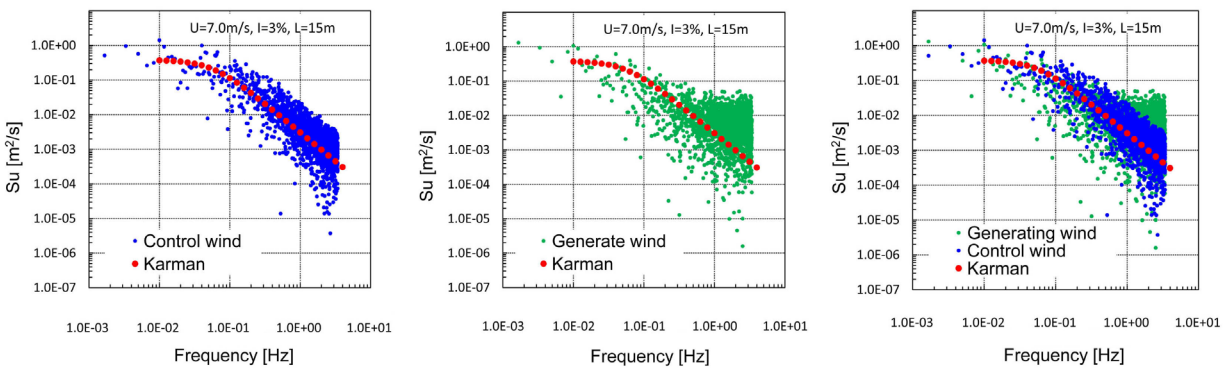


Figure 15. Comparison of PSD of control and generated wind with the turbulence grid at $U = 7.0$ m/s, $I = 3\%$ and $L = 15$ m (Left: control, middle: generated, right: composite).

4. Conclusions

This paper describes a low-cost actively controlled multi-fan wind tunnel with an original embedded system and 100 PC fans of the driving section to generate artificial natural wind through Kármán’s power spectrum density function (PSD). This wind tunnel can successfully generate two kinds of natural winds with turbulent intensities of 2% and 3% and with a mean velocity of about 7 m/s.

To this wind, we apply inverse Fast Fourier Transformation assuming a random phase to the Kármán's PSD. Winds with a turbulence intensity of 2% can be reproduced with the varying integral scale 5 m, 10 m and 20 m without the turbulence grid. Winds with a turbulence intensity of 3% can be reproduced with the varying integral scale 3 m, 6 m and 15 m with the turbulence grid. The winds with a turbulence intensity of 2% satisfy the Kolmogorov's $-5/3$ multiplication rule of inertial subrange with the frequency range from 0.01 Hz to 2.0Hz.

As a feature of this wind tunnel, the costs of the driving section are about one-tenth or less than one consisting of servo motors. Hence, it has the advantage that one can construct the driving section at a very low cost, and it is possible to construct a multi-fan turbulence wind tunnel at a low cost. Consequently, this wind tunnel is useful for laboratory-based experimental research using natural wind.

Conflicts of Interest

The authors declare no conflicts of interest regarding the publication of this paper.

References

- [1] Makita, S. (2002) Turbulence Wind Tunnel. *Nagare*, **21**, 409-418.
- [2] Nishi, A., Kikugawa, H., Matsuda, Y. and Tashiro, D. (1997) Turbulence Control in Multiple-Fan Wind Tunnels. *Journal of Wind Engineering and Industrial Aerodynamics*, **67-68**, 861-872. [https://doi.org/10.1016/S0167-6105\(97\)00124-4](https://doi.org/10.1016/S0167-6105(97)00124-4)
- [3] Nomura, T., Yamagata, T. and Kimura, K. (1998) Generation of Fluctuation of Wind Velocity and Direction Using Wind Tunnels Driven by AC Servomotors. *Proceedings of the 15th National Symposium on Wind Engineering*, 197-202.
- [4] Ozono, S., Miyagi, H. and Wada, K. (2007) Turbulence Generated in Active Grid Mode Using a Multi-Fan Wind Tunnel. *Journal of Fluid Science Technology*, **2**, 643-654.
- [5] Cao, S. and Cao, J. (2017) Toward Better Understanding of Turbulence Effects on Bridge Aerodynamics. *Frontiers Built in Environment*, **3**, 72. <https://doi.org/10.3389/fbuil.2017.00072>
- [6] Wang, J.Y., Meng, Q.H., Luo, B. and Zeng, M. (2018) A Multiple-Fan Active Control Wind Tunnel for Outdoor Wind Speed and Direction Simulation. *Review of Scientific Instruments*, **89**, Article ID: 035108. <https://doi.org/10.1063/1.5009897>
- [7] Kármán's, V.T. (1948) Progress in the Statistical Theory of Turbulence. *Proceedings of the National Academy of Sciences of the United States of America*, **34**, 530-539. <https://doi.org/10.1073/pnas.34.11.530>
- [8] Teunissen, H.W. (1980) *The Structure of Turbulent Shear Flow*. 2nd Edition, Cambridge University Press, Cambridge, 53-59.
- [9] Simiu, E. and Scanlan, R.H. (1986) *Wind Effects on Structures: An Introduction to Wind Engineering*. 2nd Edition, Wiley-Interscience, Hoboken, NJ, 48-65.
- [10] Tsuchiya, M., Ishihara, T., Fukumoto, Y., Sukegawa, H. and Okubo, K. (2006) The Wind Observation on Pacific Ocean for Offshore Wind Farm. *Proceedings of National Symposium on Wind Engineering*, **19**, 121-126.